06 December 2012

Experiments on Reverse-Channel Connections at Elevated Temperatures

Shan-Shan Huang[a,*], Buick Davison[a] and Ian W. Burgess[a]

[a] Department of Civil and Structural Engineering, The University of Sheffield, Sir Frederick Mappin Building, Mappin Street, Sheffield, S1 3JD, UK

* Corresponding author. Tel.: +44 114 222 5727; fax: +44 114 222 5700. E-mail address: s.huang@shef.ac.uk (S.-S. Huang).

Number of words: 4808

Number of figures: 12

Number of tables: 3

Abstract

This paper reports on an experimental investigation of the behaviour of reverse-channel connections between steel beams and concrete-filled tubular (CFT) columns in fire conditions. The objectives of the tests were to assess the behaviour of beam-to-column connections subject to the combinations of significant tying and shear forces and large rotations, which can arise during a building fire, and to provide test data to characterise and validate simplified temperature-dependent component-based connection models. It has been found that the reverse-channel connections not only provide a practical solution for connecting steel beams to composite columns but they also possess high ductility and strength. Such high ductility allows greater beam deformations in fire while reducing the magnitudes of the induced axial forces, thereby enhancing the fire resistance of the connections without requiring them to be stronger.

Key words: Reverse-channel connection, Concrete-filled tubular column, Robustness, Fire.

1 Introduction

Connections between columns and beams are probably the weakest elements of steel and composite steel-concrete framed buildings subject to fire, and their fractures may trigger the buckling of columns and eventually cause the disproportionate collapse of the entire building. This was clearly demonstrated by the unexpected total collapse of the 47-storey building "Seven World Trade" of the World Trade Center complex in New York City on 11 September 2001 [1]. This building withstood minor structural damage caused by debris impact from WTC1, but collapsed due to connection failure in fire. Current connection design approaches are solely based on ambient-temperature behaviour. However, under fire exposure, large normal forces and rotations can be generated in connections, due to a combination of restraint to thermal elongation and degradation of the mechanical properties of the construction materials at high temperature. It is clear that such behaviour should be taken into account in the design of connections, in order to prevent connection fractures, which could potentially cause disproportionate overall building collapse.

For ambient-temperature design, although connections are often assumed mainly to resist vertical shear forces they also have some rotational resistance characteristics. Research on connection behaviour has initially been focused on their moment-rotation characteristics [2-6] without considering concurrent forces parallel to the axis of the beam. Several recent studies [7-10] have confirmed that the presence of axial force can significantly affect a joint's structural behaviour. The effect of axial forces is more critical when steel structures are subject to fire [11-14]. Beams expand significantly due to thermal expansion, and contract when the structure cools, causing high axial thermal stresses because these movements are usually restrained by the surrounding structure. Moreover, as temperature rises, a beam will weaken and eventually lose all its bending stiffness, hanging in catenary tension between its end connections. This will generate high tensile tying forces on connections, which may cause them to fracture.

There are two ways of preventing this from happening: (i) design the connections with higher strength, which requires the strength of other structural elements (beams and columns) to be increased as well; (ii) enhance the ductility of connections, which will allow them to deform, accommodating the large axial beam deformations and so reducing their axial forces. The latter is more effective than the former; it essentially enhances the fire resistance of connections without needing them to be stronger. The reverse-channel

(connecting beams with flush endplates to channels that are welded at their toes to the outer faces of columns), has been proposed [15] as a method of connecting a steel beam to a column with access only to its outer face. The reverse channel is welded to a column in the fabrication workshop; the endplate is welded to the beam end in the conventional manner. On site the beam is positioned between the columns, and non-preloaded bolts can be installed with either hand tools or a pneumatic impact wrench, thereby fixing the endplate to the face of the reverse channel. It allows nuts and bolts to be placed and tightened on site. This paper reports a series of tests on reverse-channel connections to concrete-filled tubular (CFT) columns, subject to combinations of normal and shear forces and bending moments, at both room and elevated temperatures. It has been found that, apart from their practicality, reverse-channel connections are also extremely ductile, which enhances their robustness in fire without requiring them to be stronger. As a bonus, such high ductility does not necessitate a compromise on strength, and actually the ultimate strength of reverse-channel connections is comparable with that of flush end-plate connections.

2 Test Programme

Table 1 summarises the tests reported in this paper. These included 16 constant-temperature tests to failure of isolated joints to CFT columns, under combinations of axial and shear forces and bending moments. This series of tests is a limited parametric study, as indicated in the table, providing experimental data for the validation of component models which may then be used for more extensive parametric studies.

The test series permitted investigation of the following aspects of behaviour:

- Comparison of the performance of round and square concrete-filled structural hollow sections;
- Comparison of the effects of temperature increase between Tests 1-4 and 5-8;
- Studies of the effect of changing *channel width* onto a circular CFT in Tests 5, 6, 9, 10;
- Studies of the effect of changing *channel width* onto a square CFT in Tests 7, 8, 11, 12;

- When assessing the effect of reverse channel:tube width ratio, a single fin plate (Tests 1, 3, 5 and 7) was included as representative of the effect on the column of a very narrow channel;

- Comparison of Tests 13 and 14 with 6 to investigate the effects of *type of channel* for circular CFT;

- Comparison of Tests 15 and 16 with 8 to assess the influence of *type of channel* for square CFT.

3 Test Setup

An existing experimental setup was used, which has been described in detail in previous papers [16, 17], and only a brief description will be given here together with the alterations made to accommodate the tests reported in this paper. The tests were conducted in an electric furnace (Fig. 1) with an internal volume 1.0m^3. Full-size connections were heated until the temperatures of the exposed steel parts reached, and stabilised at, the specified temperature; they were then loaded under displacement control at constant temperature until fracture occurred. The loading system was designed to apply a combination of normal and shear forces together with moment; a combination which is realistic in connections subject to building fires.

The specimen was placed in the middle of the furnace. A support beam extended from the left-hand hole in the furnace wall, and was connected to the column via an oversized endplate. Bolts (for square CFT) or threaded bars (for circular CFT) were partially cast into the concrete infill of the composite column for these connections. Two Φ30mm Grade 316 stainless steel bars were used to provide support to the column top from the reaction frame. Except in the tests at ambient temperature, all steelwork within the furnace, except the connection itself, the column and a significant length of the beam, were protected by thermal insulation blanket. The load was applied through a linkage of three *Macalloy* bars, which were all connected at a central pin. When the jack moved downward, an inclined tensile force was applied to the beam end through the furnace bar. The angle α between the furnace bar and the axis of the beam determined the ratio of shear (parallel to the column) and tensile (normal) forces applied to the connection. The initial value of α before testing was set at 55° for all tests. To allow as much free movement of the furnace bar as

possible through the hole in the right-hand wall of the furnace, the whole specimen was tilted by 25° in the furnace.

Digital cameras, together with image processing techniques were used to measure the specimens' displacements during these high-temperature tests. The furnace has two 100mm x 200mm observation windows, one at the front and one on top. Two digital cameras conducted interval shooting (once per minute) through the two windows throughout the test. The cameras were synchronized to one another and to the data logging system. To ensure high-quality digital images, extra lighting was provided through half of each observation window into the furnace. Fig. 2 shows examples of the images taken by the two cameras. Reference marks (Φ3mm ceramic rods inserted in drilled holes) were located on the column, beam web and reverse channel. Rotations and displacements were calculated by processing the interval-shot images to trace the movements of these marks.

4 Test Specimens

Lengths of SHS250x8 or CHS244.5x8 were filled with concrete to form the CFT columns. All beams were 305×165UKB40, although their lengths were varied to ensure that the initial position of the loaded end of the beam before testing was approximately the same for all tests. The beams connected to reverse channels were further shortened (by 20mm) because the reverse-channel connections were expected to have higher ductility than the other types. A custom-made connector was bolted to the end of the beam and the load was applied to it through a hinge. All steel members were Grade S275, except for the tubular and UKC sections which were Grade S355. Differences between the actual dimensions of the steel sections and their nominal dimensions, given in the "Blue Book" [18], were negligible. Hexagon-head M20x90-8.8 screws to ISO4017 [19], hexagon M20-10 nuts to ISO4032 [20] and 20-100HV washers to ISO7091 [21] were used. All bolt holes were 22mm diameter. The cube strength of the concrete was measured on the day of testing and is reported in Table 2. Note that the concrete strengths varied between tests. This was caused by the use of two different cement types, which was not intentional. However, it was observed from the tested specimens that the CFT columns barely deformed in either the compression or the tension zone. Therefore, it can be assumed that the concrete infill of the CFTs did not experience significant deformation. Hence the effect of the concrete infill is limited, and the variation in concrete strength should not invalidate the comparison between the tests.

The beams were connected to reverse channels with a thick (20mm) endplate to ensure that the reverse channel was the most flexible and weakest component, as desired. The standard design of a flush endplate given by the "Green Book" [22] was adopted, because the behaviour of flush endplates had previously been investigated by Yu *et al.* [23]. Since the same beams were used for all tests, their endplates (including bolt gauges) were also identical. Double nuts were used to bolt the beam endplate to the reverse channel in order to preclude the possibility of thread-stripping.

Fig. 3 shows the details of a typical reverse-channel connection. Care has been taken to ensure that the design is feasible for practical installation, by leaving enough clearance for site workers to fix bolts, in particular for the specimens using circular CFT columns. To connect these circular CFT columns to the test rig, a thick reversed channel (UKPFC150X90X24) was welded to the column and connected to the support beam with six 170mm long M20-8.8 threaded bars (ISO4017) which had a positive end anchorage (50mm square washer plates) and were embedded 150mm in the concrete infill, ensuring a stiff and strong connection of the specimen to the test rig. During the tests this part of the assembly was fire-protected and thus remained very stiff compared with the tested connection. For the square CFT columns, a steel plate was welded to the column and connected to the support beam with six bolts, with the bolt heads embedded in the concrete infill.

In the study of the effect of reverse channel:tube width ratio for reverse-channel connections to CFT columns, a single fin plate was considered as one extreme (with low channel:tube width ratio) and a reverse channel as wide as the column as the other. The standard design of a fin plate given by the BCSA/SCI guidance [24] was used, as shown in Fig. 4.

5 Test Results

5.1 *Reverse-channel Connection to CFT*

The results are shown in Table 2. The ID numbers of the tests in this table correspond to those in Table 1. The cube strength of concrete on the day of testing is denoted as σ_c. The load angle α is composed of the sum of the inclinations of the axes of the beam and the furnace bar to the horizontal axis, measured photographically. It was not possible to set α to precisely the same value at the start of each test, and so the exact initial value is given in the Table as "Initial α". During each test the angle α changed progressively from its initial value,

due to the re-alignment of the loading system and the rotation of the beam itself. Its value at the end of each test is shown as "Final α". The final three columns show the maximum resultant applied force, the connection rotation at maximum resistance and the failure mode.

The test specimens were all tested to failure, except in Tests 2, 13 and 14. Test 2 was stopped when the applied load level was approaching the capacity of the test rig. In both Tests 13 and 14, the deformations of the specimens were so large that they reached the deformation capacity of the furnace (the furnace bar touched the furnace wall) before the maximum resistances were achieved.

Throughout the tests, reverse-channel connections to square and circular concrete-filled tubes (SHS250x8 and CHS244.5x8) were compared. Hot-rolled reverse channels of three different widths were tested on each type of column to investigate the effect of channel/tube width. Reverse channels of two different sizes, cut from hot-rolled SHS tubes, were also used to examine the influence of type, thickness and width/depth ratio of the reverse channel – the beam endplate connection, including the bolt spacing, remained constant. The test temperature was nominally 550°C, which was the average steel temperature for all 12 tests, except for the two "cold" tests on the widest hot-rolled reverse channel (UKPFC230x90x32) connected to the two types of CFT. This temperature was chosen on the basis of previous experience of joint testing [16, 17, 23], so that the specimens were significantly affected (the steel strength reduction factor is 0.6) but retained some strength and stiffness after heating during the tests. The target load angle α (55°) was identical for all tests. The force-rotation relationships for these tests are compared in Figs. 5 and 6 for each type of column. In these, the different line styles are used to indicate the variation in test temperature (solid for 550°C and dashed for 20°C). Note: during the initial heating prior to loading, the specimen was subject to minor compression due to the thermal restraint from the test rig which is why the forces start from small negative (compression) values.

The failure modes of the high-temperature tests using the *hot-rolled reverse channels* were identical, irrespective of the variation in column type and channel width. One example from the failed connections is shown in Fig. 7. There was no noticeable deformation in the CFT columns or in the steel beams, and neither was any damage found in the connection welds. In all cases the failure was controlled by the bolts after the reverse channel had experienced a large deformation. The web of the reverse channel was pulled outwards at the top; at the

bottom, it was pushed inwards when the channel used was wider than the beam endplate. Since the flanges of hot-rolled channel sections are significantly thicker than their webs, they remained almost straight, but moved slightly towards each other at the web-flange intersections, due to the bending deformation of the web. Unsurprisingly, these deformations of the channel web and flanges became more severe with increase of channel width. Eventually the bolts fractured in tension row by row, as indicated by the changes in the slope of the force-rotation curve (Figs. 5 and 6) in the post-peak load region. Each of the curves marked UKPFC in both figures has three changes in slope after reaching the peak load, which correspond to the sequential failures of the three bolt rows.

The ductility contributed by the reverse channel to this connection type results in very high rotational capacity without a significant compromise to ultimate strength. This is seen in Figs. 5 and 6, comparing results from this series with those from another test within the same project (on an endplate connection to a partially-encased column, tested at the same temperature) which has already been reported by the authors in [25]. Although the column types are different, these tests can be compared to one another, because the columns were almost undeformed, and because the dimensions of the specimens were similar.

When using the same size of hot-rolled reverse channel, the ultimate strength of the connection to a square column is higher than that to a circular column, but the column shape has little effect on the rotational capacity. The rotational capacity increases with increasing channel width, when connecting to the same size of column. This shows that the ductility of the connection relies mainly on the deformability of the reverse channel itself.

Fig. 8 shows the failure mode of Test 15 using a reverse channel, which was *cut from a 250 mm wide SHS tube*. Similarly to the tests using hot-rolled channels, there were no noticeable deformations in the CFT columns or in the steel beams. However, because their flanges were equal to their web thicknesses, and considerably thinner than those of the hot-rolled channels, these reverse channels provided extremely high deformability. Again, the channel web was pulled outwards, and its flanges turned inwards at the top, with deformations so large that the channel effectively unfolded. The top row of bolts eventually fractured in tension, which allowed the channel to unfold almost to a trapezoidal shape, so that the outer parts of its flanges and its web acted almost in uniaxial tension together. Cracks started to develop in the connecting welds when this large deformation took place, but no fracture occurred in the reverse channel itself. This extremely high ductility is reflected by

the nearly-doubled rotational capacity compared with the hot-rolled channels, as shown in Figs. 5 and 6. Both the ultimate resistance and rotational capacity are increased with increasing channel width and thickness, when connecting to the same size of column. This confirms that the strength and ductility of such connections are dependent mainly on the strength and deformability of the reverse channel. Narrower reverse channels, which were cut from 200 mm wide SHS tubes, were also tested. The pre-failure deformations were the same as for the tests with wider tube-cut channels, but the failure mode switched to bolt pullout (bolt heads punching through bolt holes). The comparison between the two types of column for this series of tests is not possible because the tests with circular CFT (Tests 13 and 14) had to be stopped before the specimens failed, as noted earlier.

The widest hot-rolled reverse channel (UKPFC230x90x32), connected to each type of CFT column, was also tested (Tests 2 and 4) at ambient temperature. The joint to the circular column (Test 2) did not fail because the capacity of the test rig was approached before failure occurred. The final connection rotation was 9.18°, mainly due to the deformation of the reverse channel. Its deformed shape was very similar to that seen at high temperature, as shown in Fig. 7. The failure of Test 4 is shown in Fig. 9. This was controlled by brittle fractures in the channel web around the top row of bolts, with the bolt heads punching through the bolt holes. Again, the reverse channel experienced a considerable deformation, of the same shape produced by Test 2, before this failure occurred. Although Test 2 was stopped before failure, it is clear that the ultimate strength and rotation capacity of the connections to the circular column are higher than those for comparable connections to the square column.

5.2 *Fin Plate Connection to CFT*

Table 3 shows a summary of the results of the tests on the fin plate connections. The column titles are the same as those in Table 2. The data for the first 15 minutes of Test 7 was not recorded due to a fault in the data logging system. Four tests were planned and completed. These included two tests at high temperature and two at ambient temperature.

The test specimens were all tested to failure, but Test 1 initially had to be stopped because the weld connecting the specimen to a support bar fractured before any sign of failure was seen. This weld was reinstated and the connection was reloaded. The details of the fin plates used for these four tests were the same, as described in Section 3. Throughout the

tests, fin plate connections onto square and circular concrete-filled tubes (SHS250x8 and CHS244.5x8) were compared. The two cold tests were compared with the two hot ones. In addition, these tests were compared with those on the reverse-channel connections to CFT columns, because the fin plate is considered as the lower extreme of the range of variation of the channel/tube width ratio.

At ambient temperature, the failure was controlled by the steel tube, as shown in Fig. 10. The tube fractured in the embrittled "heat-affected zone" adjacent to the connection weld, on the side contacting the beam web. After the fracture occurred, the column wall was pulled further outwards. This deformation was larger in the square column than in the circular column; the other parts of the specimens barely deformed.

At high temperature, the column shape significantly influenced the connection behaviour. As shown in Fig. 11(a), the connection to square CFT failed by fracturing the tube wall and the connection weld in tension. The top row of bolts was slightly sheared-through. There was no visible deformation in the steel beam or in the fin plate. The crack in the steel tube revealed the concrete core, which did not show any signs of damage. Compared with a square CFT, the deformability of the face of the concrete-filled circular tube was very limited, and the failure mode switched to bolt shear, as shown in Fig. 11(b). All bolts were completely sheared, while the other parts of the connection underwent noticeable deformation. This failure mode gave much lower rotational capacity for the connection than when the square CFT was used. The reason the column shape affects on the failure mode is that:

- The square column face will initially bend without creating membrane (hoop) stresses, and this will induce the highest bending moments and stresses in the embrittled heated-affected zones adjacent to the welds. This can easily initiate cracking in the column face.

- Bending of the circular column face is extremely difficult, given a circular concrete infill; increasing the enclosed area is impossible without generating tensile hoop stresses in the tube. This prevents high localized bending moments from occurring in the heat-affected zones, and prevents the cracking of the round column face.

Fig. 12 shows the force-rotation relationships for these tests. There is a sudden drop in force in the curve for the cold test on the fin plate connection to the circular CFT. This reflects the

failure of the weld connecting the specimen to one of the support bars. Since the specimen had not shown any sign of failure at this stage, this weld was reinstated and the connection was reloaded. The rotation data of the repeat test was adjusted to fit that of the initial test, from the point at which the weld failure had occurred. It can be seen from the dotted black fitted curve that, after reaching the previous peak load, the curve essentially continues unaffected. The solid black curve, representing the observed rotations, cannot be treated as more valid than this, because of the resetting that occurred due to the repair.

At ambient temperature, the load capacity of the fin plate connections onto the circular CFT is considerably higher than those for connections to the square CFT. The ultimate strength decreases dramatically with temperature rise. At high temperature, the high deformability of the face of the square tube provided very high ductility to the connection. The load capacity was not greatly affected by the variation in column shape. The rotational capacities of the fin plate connections are all lower than those of the reverse-channel connections, except the fin plate connection to square CFT tested at high temperature.

6 Conclusion

This paper presents an experimental investigation of the robustness of reverse-channel connections to CFT columns at elevated temperatures. The two key parameters studied are (i) the ultimate strength of the connection subject to the combination of tension, shear and bending moment and (ii) the rotational capacity. This series of tests served as a limited parametric study and the effects of the CFT column shape, temperature, reverse channel width and type were examined. The test results showed that:

1. the reverse channel connection provides a feasible way of connecting a steel beam to a composite column, with significantly enhanced ductility compared to the flush endplate connection, and without compromising ultimate strength;

2. fin plate connections, included as an extreme case of a very narrow reverse channel, demonstrated reasonable ductility but at a reduced strength compared with a 180mm wide rolled channel;

3. the main failure modes of the reverse channel connections were; fracture of the reverse channel web at 20°C, bolt heads punching through bolt holes (for the

narrower tube-cut channels tested at 550°C), and tensile fracture of bolts (for all UKPFC reverse channels and the wider tube-cut channels tested at 550°C);

4. the ductility of reverse channel connections could be controlled in performance-based design by varying the width/thickness ratio of the channel and the spacing of the bolts.

The test data has been used to develop a component-based connection model for the reverse-channel connection [26, 27]. This model has also been integrated into global frame analysis as a connection finite element, which not only enables practical and accurate prediction of the failure of connections to be made but also allows progressive collapse sequences to be traced, facilitating analytical performance-based design against fire.

ACKNOWLEDGMENT: *The research leading to these results has received funding from the European Community's Research Fund for Coal and Steel (RFCS) under grant agreement n° RFSR-CT-2009-00021.*

References

[1] National Institute of Standards and Technology (NIST). Final report on the collapse of world trade center building 7. USA: National Institute of Standards and Technology; 2008.

[2] Lawson RM. Behaviour of steel beam-to-column connections in fire. STRUCT ENG 1990;68(14):263-71.

[3] Leston-Jones LC, Lennon T, Plank RJ, Burgess IW. Elevated temperature moment-rotation tests on steelwork connections. Proc Instn Civ Engrs Structs & Bldgs 1997;122:410-9.

[4] Davison JB, Kirby PA, Nethercot DA. Rotational stiffness characteristics of steel beam to column connections. J Const Steel Res 1987;18:17-54.

[5] Al-Jabri KS, Lennon T, Burgess IW, Plank RJ. Behaviour of steel and composite beam-column connections in fire. J Const Steel Res 1998;46:1-3.

[6] Al-Jabri KS, Burgess IW, Lennon T, Plank RJ. Moment-rotation-temperature curves for semi-rigid joints. J Const Steel Res 2005;61:281-303.

[7] Jaspart J-P, Recent advances in the field of steel joints. Column bases and further configurations for beam-to-column joints and beam splices. Belgium: University of Liège, Department MSM; 1997.

[8] Cerfontaine F, Jaspart J-P. Analytical study of the interaction between bending and axial force on bolted joints. In: Proceedings of the 3rd European conference on steel structures; 2002. p. 997-1006.

[9] Wald F, Ŝvarc M. CTU Reports No. 2-3: Experiments with end plate joints subject to moment and normal force. Contributions to experimental investigation of engineering materials and structures. Prague: Czech Technical University; 2001.

[10] Luciano de Lima RO, Simões da Silva L, Vellasco PCG, Andrade SAL. Experimental evaluation of extended endplate beam-to-column joints subjected to bending and axial force. Eng Struct 2004; 26:1333-47.

[11] Liu TCH, Fahad MK, Davies J. Experimental investigation of behaviour of axially restrained steel beams in fire. J Const Steel Res 2002;58:1211-30.

[12] Mesquita LMR, Piloto PAG, Vaz MAP, Vila Real PMM. Experimental and numerical research on the critical temperature of laterally unrestrained steel I beam. J Const Steel Res 2005;61:1435-46.

[13] Simões da Silva L, Santiago A, Vila Real P, Moore DB. Behaviour of steel joints under fire loading. Steel Compos Struct 2005;5(6):485-513.

[14] Wang Y, Dai X, Bailey C. An experimental study of relative structural fire behaviour and robustness of different types of steel joint in restrained steel frames. J Constl Steel Res 2011;67(7):1149-63.

[15] Ding J, Wang YC. Experimental study of structural fire behaviour of steel beam to concrete filled tubular column assemblies with different types of joints. Eng Struct 2007;29(12):3485-502.

[16] Yu HX, Burgess IW, Davison JB, Plank RJ. Experimental investigation of the behaviour of fin plate connections in fire. In: Proceedings of the 3rd international conference on steel and composite structures; 2007. p. 541-8.

[17] Yu HX, Burgess IW, Davison JB, Plank RJ. Experimental investigation of the behaviour of fin plate connections in fire. J Constr Steel Res 2009; 65(3):723-36.

[18] Steel Construction Institute (SCI), The British Constructional Steelwork Association Limited (BCSA). P363 - Steel building design: design data, in accordance with Eurocodes and the Uk national annexes. UK: SCI, BCSA; 2009.

[19] British Standard Institute (BSI). BS EN ISO4017: Hexagon head screws - Product grades A and B. London: BSI; 2001.

[20] British Standard Institute (BSI). BS EN ISO4032: Hexagon nuts - Product grades A and B. London: BSI; 2001.

[21] British Standard Institute (BSI). BS EN ISO7091: Plain washers - Normal series - Product grade C. London: BSI; 2000.

[22] Steel Construction Institute (SCI), The British Constructional Steelwork Association Limited (BCSA). P207 - Joints in steel construction: moment connections. UK: SCI, BCSA; 1995.

[23] Yu HX, Burgess IW, Davison JB, Plank RJ. Experimental and numerical investigations of the behaviour of flush endplate connections at elevated temperatures. J Struct Eng-ASCE 2011; 137(1):80-7.

[24] Steel Construction Institute (SCI), The British Constructional Steelwork Association Limited (BCSA). P212 - Joints in steel construction: simple connections. UK: SCI, BCSA; 2002.

[25] Huang S-S, Davison JB, Burgess IW. High-temperature tests on joints to steel and partially-encased h-section columns. J Constr Steel Res 2013; 80:243-51.

[26] Burgess IW, Davison JB, Dong G, Huang S-S. The role of connections in the response of steel frames to fire, Struct Eng Int 2012; 22(4):449-61.

[27] Dong G, Burgess IW, Davison JB. Application of a general component-based connection element in structural fire analysis. In: Proceedings of the 11th International conference on steel, space and composite structures; 2012. p. xx-xx.

Figure Captions

Table Captions

Table 1 The test programme.

Table 2 Results of the tests on the reverse-channel connections to CFT columns.

Table 3 Results of the tests on the fin plate connections to CFT columns.

Table1
Click here to download Table: Table1.docx

No.	Column	Temperature (°C)	Connection Type
1	○ CFT	20	Fin plate
2	○ CFT	20	UKPFC[1]230x90x32
3	□ CFT	20	Fin plate
4	□ CFT	20	UKPFC230x90x32
5	○ CFT	550	Fin plate
6	○ CFT	550	UKPFC230x90x32
7	□ CFT	550	Fin plate
8	□ CFT	550	UKPFC230x90x32
9	○ CFT	550	UKPFC200x90x30
10	○ CFT	550	UKPFC180x90x26
11	□ CFT	550	UKPFC200x90x30
12	□ CFT	550	UKPFC180x90x26
13	○ CFT	550	RC[2] cut from SHS250x8
14	○ CFT	550	RC cut from SHS200x6
15	□ CFT	550	RC cut from SHS250x8
16	□ CFT	550	RC cut from SHS200x6

[1] UK parallel flange channel

[2] Reverse channel

Table 1 The test programme.

Table 2
Click here to download Table: Table2_v2.docx

No.	Column Shape	Temp (°C)	Reverse Channel	σ_c (MPa)	Initial α (°)	Final α (°)	Force (kN)	Rotation (°)	Failure Mode[1]
2	O	20	UKPFC230x90x32	23	50.29	37.54	254.35	9.18	No failure[2]
6	O	550	UKPFC230x90x32	45	54.62	36.73	98.45	13.27	A
9	O	550	UKPFC200x90x30	26	51.37	31.35	113.15	10.46	A
10	O	550	UKPFC180x90x26	30	53.36	34.68	112.72	9.40	A
13	O	550	Cut from SHS250x8	46	55.04	37.34	109.33	20.39	Possibly A[2]
14	O	550	Cut from SHS200x6	50	53.17	35.45	102.29	15.66	Possibly B[2]
4	□	20	UKPFC230x90x32	57	52.78	38.39	239.28	8.74	B + C
8	□	550	UKPFC230x90x32	52	55.37	36.79	126.13	12.21	A
11	□	550	UKPFC200x90x30	57	56.41	35.28	120.49	9.76	A
12	□	550	UKPFC180x90x26	58	54.25	33.46	130.02	9.50	A
15	□	550	Cut from SHS250x8	59	56.59	29.53	131.54	23.02	A
16	□	550	Cut from SHS200x6	48	51.64	27.00	109.03	19.54	B

[1] Failure modes:

A: tensile fracture of bolts

B: bolt pullout (bolt heads punching through bolt holes)

C: fracture of the reverse channel web

[2] No failure (technical limitation)

Table 2 Results of the tests on the reverse-channel connections to CFT columns.

Table3
Click here to download Table: Table3.docx

No.	Column Shape	Temperature (°C)	σ_c (MPa)	Initial α (°)	Final α (°)	Force (kN)	Rotation (°)
1	O	20	52	55.50	41.66	189.53	8.49
3	□	20	71	53.65	41.48	143.73	8.55
5	O	550	42	52.97	33.40	71.35	7.06
7	□	550	67	-	43.64	67.88	12.20

Table 3 Results of the tests on the fin plate connections to CFT columns.

Figure1
Click here to download Figure: Fig1.docx

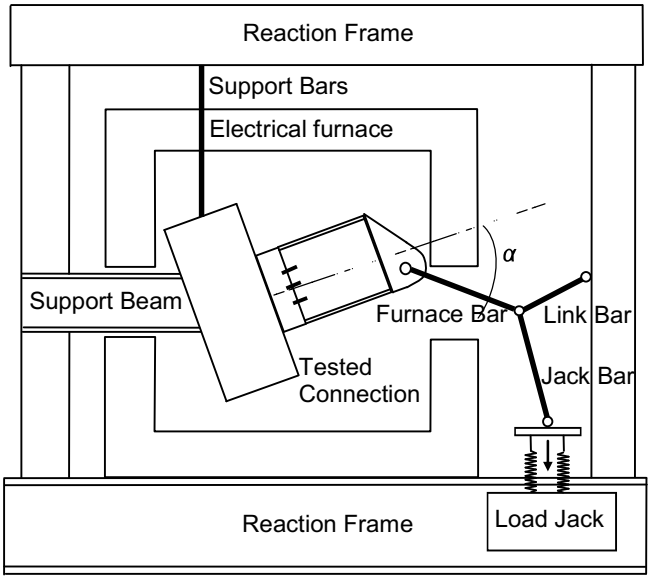

Fig. 1 The test setup.

Figure2
Click here to download Figure: Fig2.docx

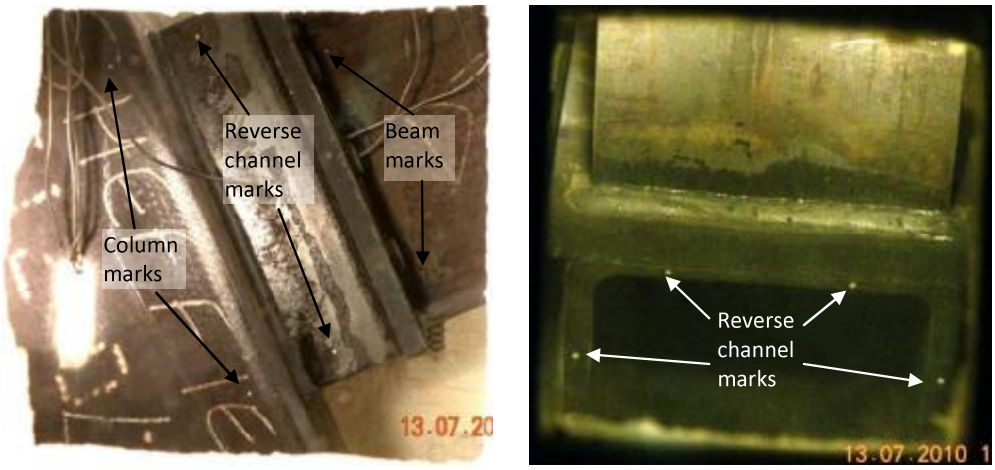

(a). View from the front window (b). View from the top window

Fig. 2 Camera measurement of the specimen deformation.

Figure3
Click here to download Figure: Fig3.docx

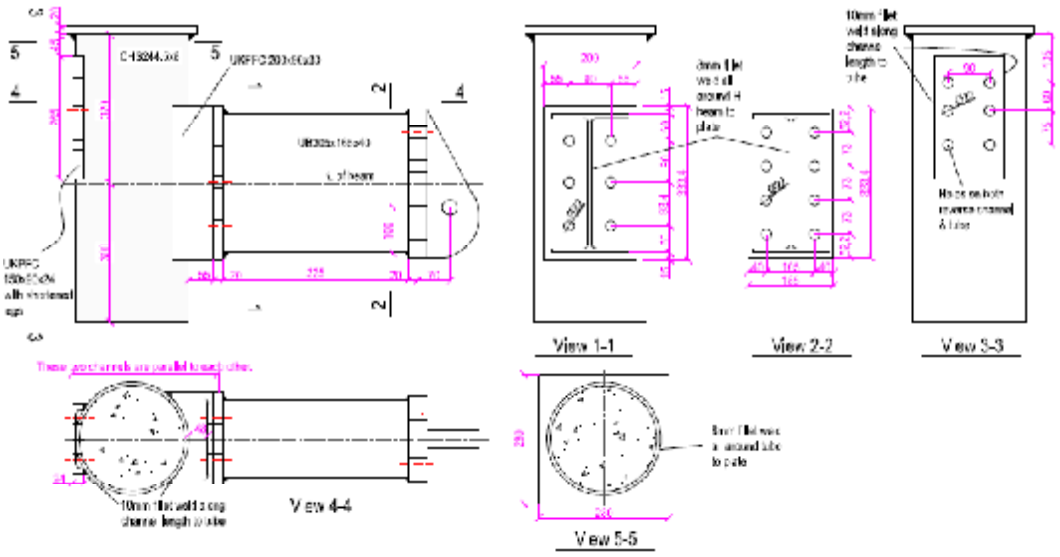

Fig. 3 Geometry of a typical reverse-channel connection to circular CFT column.

Figure4
Click here to download Figure: Fig4.docx

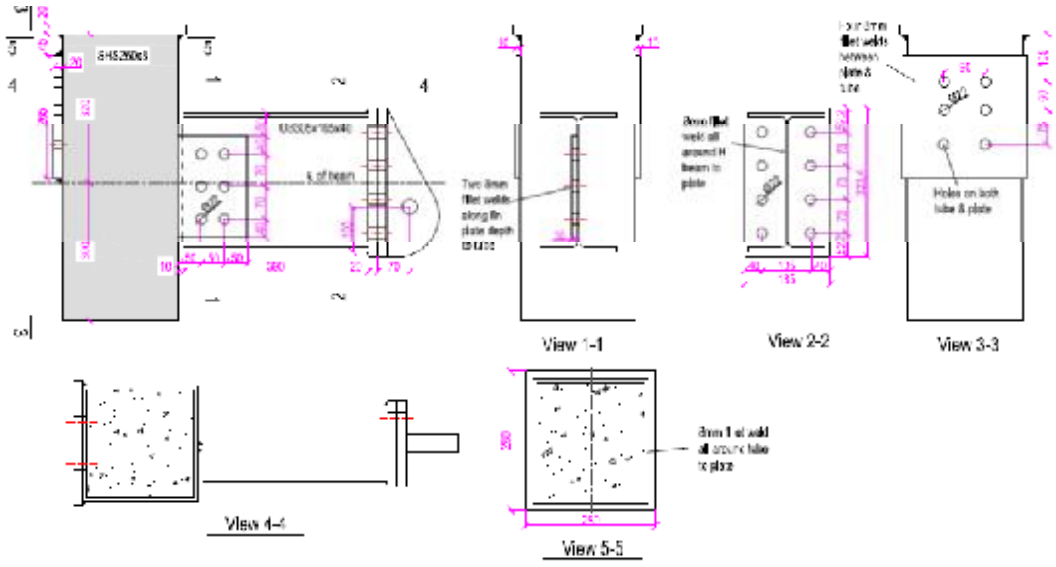

Fig. 4 Geometry of a typical fin plate connection.

Figure 5
Click here to download Figure: Fig5_v2.docx

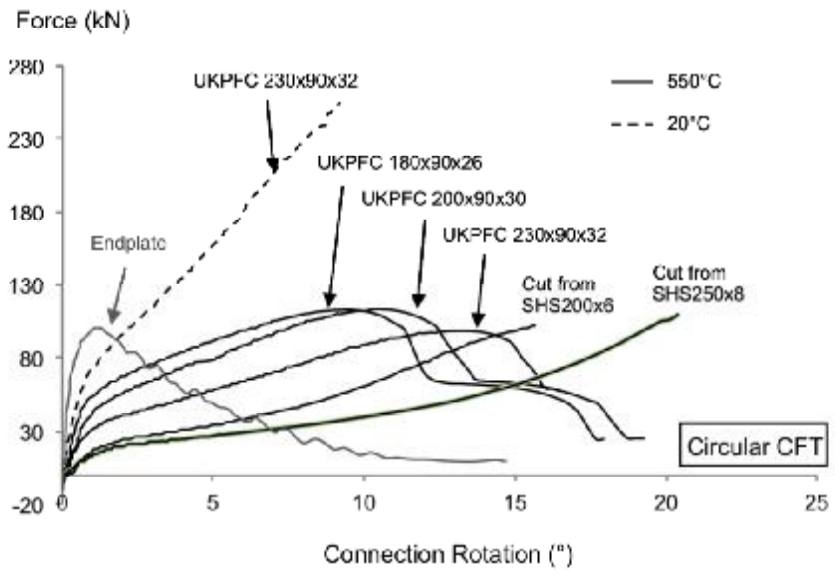

Fig. 5 The force-rotation relationships of the reverse-channel connections to circular CFT columns compared to that of the endplate connection to partially-encased column.

Figure 6
Click here to download Figure: Fig6_v2.docx

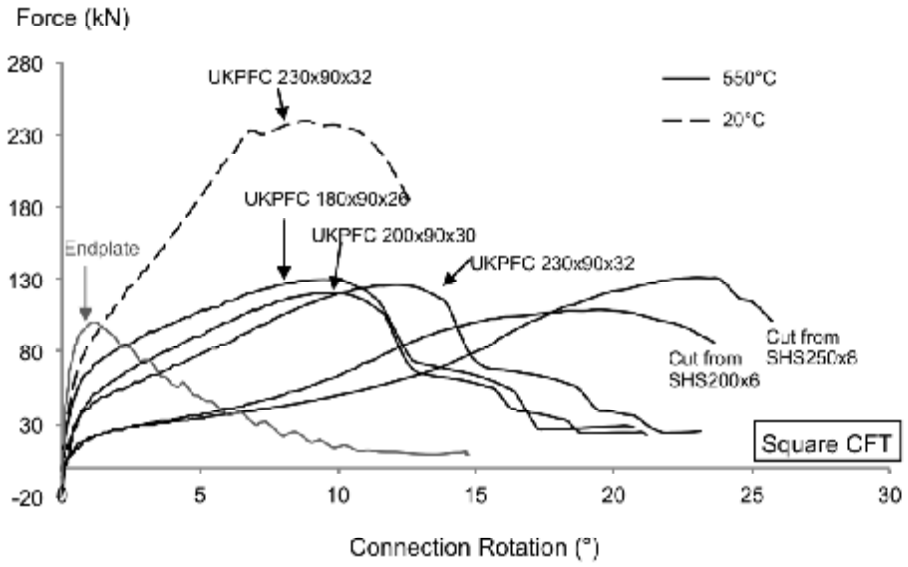

Fig. 6 The force-rotation relationships of the reverse-channel connections to square CFT columns compared to that of the endplate connection to partially-encased column.

Figure7
Click here to download Figure: Fig7.docx

Fig. 7 Failure mode of Test 8.

Figure 8
Click here to download Figure: Fig8_v2.docx

Fig. 8 Photographs after Test 15.

Figure9
Click here to download Figure: Fig9.docx

Fig. 9 Post-test photographs of Test 4.

Figure10
Click here to download Figure: Fig10.docx

(a). Connected to square CFT

(b). Connected to round CFT

Fig. 10 Failure of the fin plate connections at ambient temperature.

Figure11
Click here to download Figure: Fig11.docx

(a). Connected to square CFT

(b). Connected to circular CFT

Fig. 11 Failure of the fin plate connections at 550°C.

Figure 12
Click here to download Figure: Fig12_v3_Final.docx

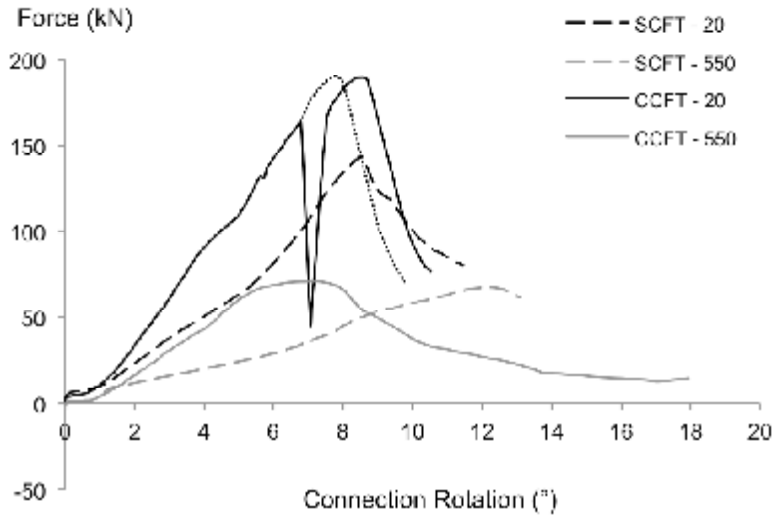

Legend: column type - test temperature in °C

Fig. 12 The force-rotation relationships of the fin plate connections.